Anaphase A Chromosome Movement and Poleward Spindle Microtubule Flux Occur At Similar Rates in *Xenopus* Extract Spindles

Arshad Desai,*‡ Paul S. Maddox,*§ Timothy J. Mitchison,*‖ and E.D. Salmon*§

*Marine Biological Laboratory, Woods Hole, Massachusetts; ‡Department of Biochemistry and Biophysics, University of California, San Francisco, California; §Department of Biology, University of North Carolina, Chapel Hill, North Carolina; and ‖Department of Cell Biology, Harvard Medical School, Boston, Massachusetts

Abstract. We have used local fluorescence photoactivation to mark the lattice of spindle microtubules during anaphase A in *Xenopus* extract spindles. We find that both poleward spindle microtubule flux and anaphase A chromosome movement occur at similar rates (~2 μm/min). This result suggests that poleward microtubule flux, coupled to microtubule depolymerization near the spindle poles, is the predominant mechanism for anaphase A in *Xenopus* egg extracts. In contrast, in vertebrate somatic cells a "Pacman" kinetochore mechanism, coupled to microtubule depolymerization near the kinetochore, predominates during anaphase A. Consistent with the conclusion from fluorescence photoactivation analysis, both anaphase A chromosome movement and poleward spindle microtubule flux respond similarly to pharmacological perturbations in *Xenopus* extracts. Furthermore, the pharmacological profile of anaphase A in *Xenopus* extracts differs from the previously established profile for anaphase A in vertebrate somatic cells. The difference between these profiles is consistent with poleward microtubule flux playing the predominant role in anaphase chromosome movement in *Xenopus* extracts, but not in vertebrate somatic cells. We discuss the possible biological implications of the existence of two distinct anaphase A mechanisms and their differential contributions to poleward chromosome movement in different cell types.

A major focus in the study of cell division is to define the physical mechanisms that segregate replicated chromosomes to daughter cells. Both mitotic and meiotic cells assemble a bipolar, microtubule (MT)[1]-based spindle to execute chromosome segregation. The primary site for attachment of chromosomes to the spindle MTs is the kinetochore—a nucleoprotein structure formed at the primary constriction of mitotic chromosomes (Rieder and Salmon, 1998). During spindle assembly, kinetochores capture the plus ends of dynamically unstable MTs associated with opposite spindle poles, and become tethered to the poles by forming a stable bundle of kinetochore MTs (kMTs). After all the chromosomes are properly attached, the connections holding the sister chromatids (mitosis, meiosis II) or homologous chromosomes (meiosis I) are dissolved and the separated chromosomes move toward opposite spindle poles. Segregation of sisters to daughter cells involves both chromosome-to-pole movement (anaphase A) and spindle pole-to-pole elongation (anaphase B).

An important issue in the study of chromosome segregation is defining the mechanism of anaphase A chromosome-to-pole movement. The most popular model for anaphase A is the "Pacman" kinetochore model, which postulates that the kinetochore pulls the chromosome poleward on relatively stationary kMTs and this movement is coupled to depolymerization of the kMTs at the kinetochore (Fig. 1 *A*; for reviews see Rieder and Salmon, 1994, 1998; Yen and Schaar, 1996). The popularity of this model is derived in large part from the identification of the kinetochore as the primary site of kMT disassembly dur-

Address all correspondence to Arshad Desai, 240 Longwood Avenue, Bldg. C-517, Department of Cell Biology, Harvard Medical School, Boston, MA 02115. Tel.: (617) 432-2688. Fax: (617) 432-3702. E-mail: Arshad_Desai@ hms.harvard.edu

After June 15, 1998, Arshad Desai's present address will be EMBL, Meyerhofstrasse 1, Heidelberg 69117, Germany. Tel.: 49-6221387337. Fax: 49-6221387306.

The real time data presented in this paper can be viewed at http://skye.med.harvard.edu/movies/anaphase.html

1. *Abbreviations used in this paper*: MT, microtubule; kMT, kinetochore microtubule; nonkMT, nonkinetochore microtubule; C2CF, bis-caged carboxyfluorescein; AMPPNP, 5′-adenylylimidodiphosphate; DAPI, 4′,6′-diamidino-2-phenylindole; CSF, cytostatic factor.

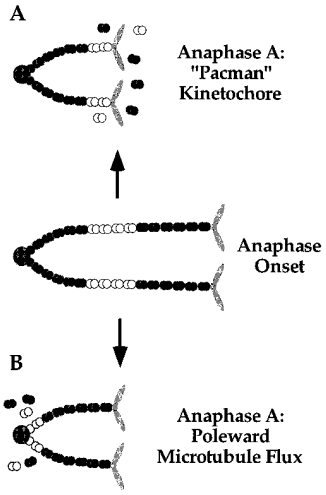

Figure 1. Two models for anaphase A chromosome-to-pole movement. For simplicity, only one half of the bipolar spindle and one kMT connecting the kinetochore to the spindle pole are shown. (*A*) *"Pacman" kinetochore*, kinetochores pull the chromosome poleward on relatively stationary kMTs coupled to kMT disassembly at the kinetochore. (*B*) *Poleward Microtubule Flux* ("traction fiber"), poleward flux of kMTs pulls chromosomes poleward coupled to kMT disassembly near the pole. The two models can be distinguished by making a fluorescent mark on the kMTs (indicated by the lighter subunits) between the kinetochore and the spindle pole and monitoring the behavior of the mark as the chromosomes move poleward.

ing chromosome-to-pole movement in vertebrate somatic cells (Mitchison et al., 1986; Wadsworth and Salmon, 1986; Gorbsky et al., 1987, 1988; Mitchison and Salmon, 1992; Zhai et al., 1995; Waters et al., 1996).

Another model for anaphase A chromosome movement postulates that kinetochores are pulled poleward by the poleward movement or "flux" of kMTs coupled to depolymerization of kMT minus ends near the poles (Fig. 1 *B*). According to this model, kMTs flux poleward (or treadmill, see Margolis and Wilson, 1981) during metaphase concurrent with plus end assembly at the kinetochores and minus end disassembly near the poles. In anaphase, assembly stops at the kinetochore and the poleward movement of the kMTs coupled to their minus end disassembly pulls the kinetochore and its associated chromosome poleward (Fig. 1 *B*). Related "traction fiber" models have been proposed by Inoué and Sato (1967), Forer (1965, 1966), Margolis and Wilson (1981), and others (for reviews see Fuge, 1989; Salmon, 1989), primarily on the basis of indirect evidence for poleward MT transport, including observations that various types of organelles, "particles or states" and UV ablation zones in spindle fibers move poleward during both metaphase and anaphase.

Mitchison (1989) provided direct evidence for poleward MT flux by using fluorescence photoactivation to locally mark the lattice of kinetochore fiber MTs in mitotic PtK2 cells. Fluorescent marks on the kMTs moved poleward at an average rate of 0.5 μm/min during metaphase with plus end assembly near the kinetochore being balanced by minus end disassembly near the poles. Subsequent fluorescence photoactivation analysis of the sites of kMT disassembly during anaphase in newt, PtK1, and porcine somatic cells has shown that the majority of kMT disassembly during chromosome-to-pole movement occurs at the kinetochore (Mitchison and Salmon, 1992; Zhai et al., 1995; Waters et al., 1996). In these cell types, chromosome-to-pole movement (1.5–2.5 μm/min) is much faster than anaphase poleward kMT flux (0.3–0.5 μm/min). Thus, during anaphase, fluorescent marks made on kMTs near the kinetochore disappear because kinetochore poleward movement coupled to kMT disassembly at the kinetochore is three to eight times faster than the rate of poleward flux coupled to kMT disassembly at the poles. Waters et al. (1996) have shown in newt lung cells that, if MT assembly and disassembly at the kinetochore are blocked during anaphase by taxol concentrations that do not inhibit kMT poleward flux, then chromosomes are pulled poleward slowly at kMT flux rates. Taken together, these studies have led to the conclusion that, although poleward MT flux is capable of generating force to move chromosomes, it is only a minor contributor to anaphase A chromosome movement in vertebrate somatic cells.

The marking studies in somatic cells raise the question as to what is the function of poleward MT flux—a concerted dynamic behavior of spindle MTs that reflects considerable structural complexity in the spindle. One possibility is that MT flux is the dominant mechanism for poleward chromosome movement in systems other than vertebrate somatic cells. Sawin and Mitchison (1991) found that the majority of MTs in spindles assembled in meiosis II metaphase-arrested *Xenopus* egg extracts flux poleward at 2.9 ± 0.4 μm/min, approximately six times faster than the rate of kMT poleward flux in somatic cells. Forer and co-workers found that in insect meiocytes both zones of reduced birefringence generated by UV ablation of spindle MTs (Forer, 1965, 1966) and acetylated tubulin distributions along kinetochore fibers (Wilson et al., 1994) move poleward at rates similar to chromosomes during anaphase A; however, interpretation of these two studies is complicated by the fact that the first involved cutting spindle MTs, and the second involved extrapolating dynamic information from fixed samples. Nevertheless, these three observations suggest that poleward MT flux may play the predominant role in anaphase A chromosome movement in certain systems. Consistent with the flux hypothesis, direct observations of anaphase in *Xenopus* extract spindles showed that chromosomes move poleward at 2.4 ± 1 μm/min (Murray et al., 1996), within the range of values observed for poleward MT flux during metaphase in this system (Sawin and Mitchison, 1991). However, Mitchison and Salmon (1992) showed in newt lung cells that the rate of kMT poleward flux during early anaphase is similar to that during metaphase, but slows down significantly in late anaphase. A subsequent study on porcine and marsupial somatic cells showed that kMT flux in these cell types was ~50% slower during anaphase than during metaphase (Zhai et al., 1995). Since these somatic cell studies demonstrated changes in the flux rate between metaphase and anaphase, determining whether poleward MT flux plays the predominant role during anaphase A in *Xenopus* extract spindles requires simultaneous observation of MT flux and anaphase chromosome movement.

In this paper, we have used fluorescence photoactivation to mark the lattice of spindle MTs during anaphase in *Xenopus* extract spindles. We have directly compared the rate of poleward flux to the rate of poleward chromosome movement and find that both the spindle MT lattice and the disjoined chromosomes move poleward at ~2 μm/min under our experimental conditions. We also show that anaphase A in the extract spindles exhibits a distinct phar-

macological profile from anaphase A in somatic cell spindles, and that the extract spindle profile is consistent with a predominantly MT flux–driven mechanism for moving chromosomes poleward.

Materials and Methods

In Vitro Spindle Assembly

All experiments were performed using fresh cytostatic factor (CSF)-arrested *Xenopus* egg extracts prepared as described (Murray, 1991; Desai et al., 1998). Extracts were supplemented with 5–10 μg/ml X-rhodamine tubulin, 200–400 permeabilized sperm nuclei/μl and bipolar spindles were assembled as described (Shamu and Murray, 1992; Murray et al., 1996; Desai et al., 1998). Briefly, calcium was added to a final concentration of 0.4 mM (from a 10× [4 mM] stock in sperm dilution buffer (SD) (10 mM Hepes, pH 7.7, 100 mM KCl, 1 mM $MgCl_2$, 150 mM sucrose, 10 μg/ml cytochalasin D) to CSF extract containing sperm nuclei, incubated at room temperature (20°–23°C) for 80 min to allow the sperm DNA to decondense and replicate, after which 20 μl of CSF extract (without any sperm nuclei but with X-rhodamine tubulin) was added to drive the reactions into metaphase. To maximize the time of use of an extract for real-time experiments, we stored CSF extracts on ice after preparation and started a new set of spindle assembly reactions every 3–3.5 h. There is significant day-to-day variability in both the lifetime and anaphase competency of these extracts, which considerably limits experimental manipulations.

X-rhodamine tubulin and bis-caged carboxyfluorescein (C2CF) tubulin were prepared using the high pH tubulin labeling protocol (Hyman et al., 1991; Desai and Mitchison, 1998). The C2CF tubulin used in these experiments was labeled to a stoichiometry of ~0.8 moles C2CF/mole tubulin. H1 kinase assays were performed as described (Murray, 1991).

Sample Preparation for Real Time Analysis

Slides and coverslips were cleaned using water, acetone, and ethanol sequentially as described (Murray et al., 1996; Desai et al., 1998). For marking experiments, C2CF tubulin was added at least 10 min before starting anaphase to a final concentration of 100–150 μg/ml. All steps involving C2CF tubulin were performed under dim red illumination in a dark room. For simultaneous observation of poleward flux and chromosome-to-pole movement, the 10× calcium stock in SD was supplemented with 5 μg/ml 4,6-diamidino-2-phenylindole (DAPI) (Ca/DAPI5). 1:9 vol of Ca/DAPI5 was added to a reaction supplemented with C2CF tubulin and 8 μl of this mixture were pipetted onto a clean slide, covered using a clean 22 × 22-mm coverslip, and then sealed using Valap (1:1:1 vaseline/lanolin/paraffin). Sample preparations with large visible air bubbles were discarded. The submillimolar concentration of calcium added to the extract to initiate anaphase was sequestered within 1 min to basal levels, as measured using Fluo-3 (Molecular Probes, Inc., Eugene, OR) calcium fluorimetry (not shown). The calcium pulse did not appear to have a significant effect on assembled spindles since their morphology and MT density remained typical of metaphase until 5–10 min after calcium addition when anaphase chromosome segregation began.

For anaphase pharmacology studies, various 10× calcium stocks were prepared in SD containing 4 mM $CaCl_2$, 1 μg/ml DAPI, and 10× concentration of the desired dosage of a specific pharmacological agent. For flux pharmacology studies, DAPI was omitted from the stocks. Analysis of the effect of taxol on flux was performed on metaphase spindles. An analysis of the effect of 5′-adenylylimidodiphosphate (AMPPNP) on flux was done previously on metaphase *Xenopus* extract spindles (Sawin and Mitchison, 1991). Our analysis of the effect of AMPPNP on flux was done on anaphase spindles. Samples for pharmacology studies were prepared as described above, with a specific 10× stock being used to deliver a pharmacological agent.

Microscopy and Data Analysis

Photoactivation experiments were performed on an upright Photoscope III (Carl Zeiss Inc., Thornwood, NY) with a rotating stage and 60×, 1.4 NA PlanApo objective. Spindles were located at low magnification and aligned with respect to the photoactivation beam using phase contrast microscopy. Modifications of the microscope for photoactivation and for acquisition and storage of images at multiple wavelengths have been described (Sawin and Mitchison, 1991, 1994; Mitchison et al., 1998). 100-W mercury arcs were used for both illumination and photoactivation, and a SIT video camera (Dage-MTI, Wabash, WI) was used to acquire eight frame-averaged images in the fluorescein and X-rhodamine channels. Illumination intensity was controlled using a combination of an out of focus (epi-condenser) diaphragm and neutral density filters. To avoid activation of the C2CF tubulin, DAPI illumination was carefully limited by closing down the out of focus diaphragm, leaving the UV turning mirror to guide the photoactivation beam (Mitchison, 1989; Mitchison et al., 1998) in the epi-illumination light path, and acquiring only two video frames per time point in the DAPI channel. Only the residual UV, not bounced out of the epifluorescence light path by the UV turning mirror, contributed to the DAPI excitation. The amount of DAPI, X-rhodamine tubulin, and C2CF tubulin added to extracts was empirically optimized to allow image acquisition in all three channels at constant camera gain and black level. Images at each wavelength were acquired 5-s apart, and sequential images at a specific wavelength were acquired 20–30-s apart. Images were stored on optical disks using a optical memory disc recorder (TQ 3038F; Panasonic, Secaucus, NJ) and digitized for analysis using a Metamorph Imaging System (Universal Imaging Corp., West Chester, PA).

For each digitized sequence, the peak of fluorescence in the fluorescein channel (photoactivated C2CF tubulin) and the leading edge of fluorescence in the DAPI channel (marking the leading edges of the chromosomes) were defined from fluorescence intensities measured using a 5-pixel-wide linescan that was oriented along the trajectory of poleward chromosome movement and extended past the polar edge of the spindle. This linescan was also positioned such that distinct regions of photoactivated C2CF tubulin and DAPI-labeled chromosomes could be monitored through most of the duration of anaphase A. At each time point, the intensity values in each fluorescence channel along this linescan were transferred to an Excel spreadsheet. The spindle pole was defined for each time point in the X-rhodamine channel by the position of the drop-off in fluorescence intensity at the polar edge of the spindle. The change in the distance at 30–60-s intervals between the pole defined in the X-rhodamine channel and the peak of fluorescein fluorescence was used to measure flux rate and similarly the change in distance between the pole and the leading edge of DAPI fluorescence was used to measure chromosome movement rate. When feasible, rates were obtained from several linescans (two to four) through different regions of a spindle. These were generally similar to each other and their average value was used.

Given the considerable technical difficulty of simultaneous observations of poleward MT flux and anaphase chromosome movement in *Xenopus* extract spindles, analysis of the effects of pharmacological agents were performed independently for flux and chromosome movement. The photoactivation experiments were done as described above, except that the relatively tricky visualization of DAPI-labeled chromosomes was omitted. Analysis of anaphase chromosome movement was performed on a multiwavelength epifluorescence microscope described previously (Salmon et al., 1994, 1998). For these experiments, extracts were supplemented with X-rhodamine tubulin to 30–50 μg/ml and images in the X-rhodamine and DAPI channels were acquired at 30-s intervals using a Nikon 20×, 0.7 NA fluor objective (Murray et al., 1996). The movements of chromosomes at the metaphase plate were recorded at high magnification using a Nikon 60×, 1.4 NA objective. Using the Metamorph software, color overlays of the X-rhodamine and DAPI images were analyzed to determine chromosome-to-pole movement rates as described previously (Murray et al., 1996).

Fixation and Immunofluorescence of Spindles During Anaphase

To detect kinetochore antigens during anaphase chromosome movement in vitro, 20 μl of a spindle assembly reaction were diluted into 2 ml of BRB80 (80 mM K-Pipes, pH 6.8, 1 mM $MgCl_2$, 1 mM EGTA) + 30% (vol/vol) glycerol + 0.5% Triton X-100 at room temperature, mixed gently by inversion for 30–60 s, and then fixed by addition of 2 ml of BRB80 + 0.5% Triton X-100 + 30% (vol/vol) glycerol + 5% formaldehyde for ~10 min at room temperature. The fixed reactions were layered onto a 4-ml cushion of 40% (vol/vol) glycerol in BRB80 and sedimented at 5,500 rpm for 20 min at 16°C in an HS-4 rotor. After centrifugation, the sample was aspirated until just below the sample–cushion interface, rinsed with BRB80, and then the cushion was aspirated before transferring the coverslips to a coverslip holder. The coverslips were briefly rinsed in TBSTx (20 mM Tris-Cl, pH 7.4, 150 mM NaCl, 0.1% Triton X-100) to remove residual glycerol, postfixed using −20°C methanol, rehydrated in TBSTx, and then

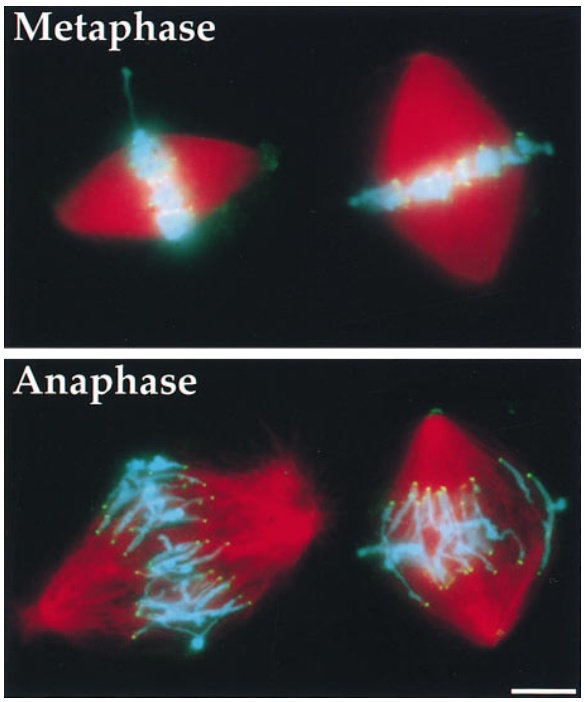

Figure 2. Immunofluorescence micrographs of fixed spindles showing that kinetochores lead chromosomes-to-pole movement during anaphase in *Xenopus* extract spindles. Spindle MTs are stained red using rhodamine tubulin, chromosomes are stained blue by DAPI and CENP-E is stained green using an anti–CENP-E primary and fluorescein-labeled secondary antibodies. Metaphase-arrested bipolar spindles with replicated chromosomes contained tight metaphase plates with sister kinetochores of bivalent chromosomes localized to the equatorial region of the spindle (*top*). Addition of a pulse of calcium to the extract inactivated the metaphase arrest and 8 min after calcium addition separated sister chromatids were seen moving poleward (*bottom*). Discrete foci of CENP-E are clearly visible at the leading edges of the poleward-migrating chromosomes. Bar, 10 μm.

processed for anti–CENP-E immunofluorescence using a cross-reactive anti–human CENP-E antibody as described (Desai et al., 1997).

Results

Poleward Microtubule Flux and Chromosome Movement Occur at Similar Rates in Xenopus Egg Extract Spindles

Metaphase-arrested in vitro spindles containing replicated chromosomes were induced into anaphase by addition of a pulse of calcium to inactivate the CSF metaphase arrest, as described by Murray and co-workers (Shamu and Murray, 1992; Murray et al., 1996). These previous studies showed that sister chromatids segregate under these conditions, but did not analyze the role of kinetochores in the observed segregation. To determine if poleward force on chromosomes during anaphase in vitro acts at their kinetochores, we examined the distribution of a known kinetochore protein. We found that CENP-E, a conserved kinetochore-localized MT motor in vertebrates (Yen et al., 1992; Desai et al., 1997; Wood et al., 1997), localizes to the leading edges of the poleward-moving chromosomes in anaphase (Fig. 2). Furthermore, during poleward movement the leading edges of chromosomes are often seen close to one end, consistent with the fact that many *Xenopus* chromosomes are "acrocentric" (i.e., have their centromeres near one end of the chromosome) (Graf and Kobel, 1991). Thus, kinetochores of in vitro spindles contain a conserved kinetochore MT motor protein and lead the chromosomes poleward in anaphase.

To directly compare the rate of chromosome poleward movement to that of spindle MT flux, we imaged both processes simultaneously using multiwavelength time lapse fluorescence microscopy. To visualize spindle structure, we added X-rhodamine–labeled tubulin to the extract immediately after preparation. To visualize poleward MT flux, we added caged fluorescein tubulin to metaphase spindles 10–30 min before inducing anaphase. Both modified tubulins rapidly equilibrate into spindle MTs as a result of MT turnover (Sawin and Mitchison, 1991). Since UV illumination photolyses caged fluorescein, activating its fluorescence, we initially avoided using UV-excited, DNA-binding dyes to visualize chromosome movement. Instead, we attempted to use phase contrast microscopy, a method that was successful for similar studies in somatic cells. However, we found that chromosomes formed in vitro in *Xenopus* extracts lack sufficient phase density, relative to extract cytoplasm, to allow reliable tracking of their movement. Therefore, we developed conditions using minimal UV-excited DAPI fluorescence that allowed us to visualize chromosomes without causing significant uncaging of caged fluorescein. Using these conditions, we recorded spindles until they had just begun anaphase chromosome movement (~8–12 min after calcium addition), then used a brief (1–3-s duration) slit of UV illumination to fluorescently mark the MTs between the poleward-migrating chromosomes and a spindle pole. The subsequent movement of the fluorescent mark, the chromosomes and changes in spindle structure were recorded.

The result of an anaphase marking experiment performed using this procedure is shown in Fig. 3 *A*. In this experiment, the mark was made just to the left of the leading edges of the chromosomes as they started to move poleward. As shown in the middle column of Fig. 3 *A*, the fluorescent mark moved poleward during the next 5 min at a rate of ~2 μm/min. Since the spindle pole-to-pole distance did not change significantly during this period, the movement of the mark must represent disassembly of the spindle MTs at their minus ends near the pole. During the same period the chromosomes moved poleward (Fig. 3 *A*, *left* and *right columns*). The striking correspondence between the poleward movement of the chromosomes and the fluorescent mark is evident in the right column of Fig. 3 *A*.

To analyze the data generated by such an experiment, we used fluorescence linescan intensity profiles along the same 5-pixel-wide linescan in all three channels to track chromosome leading edge-to-pole and peak of fluorescent mark intensity-to-pole distances as a function of time. As shown in Fig. 3 *B*, the movement of the fluorescent mark polewards closely parallels the movement of the leading edge of the chromosome mass (indicated by a dot in the linescan profile). The similarity of the average rates of anaphase poleward flux and anaphase chromosome movement from

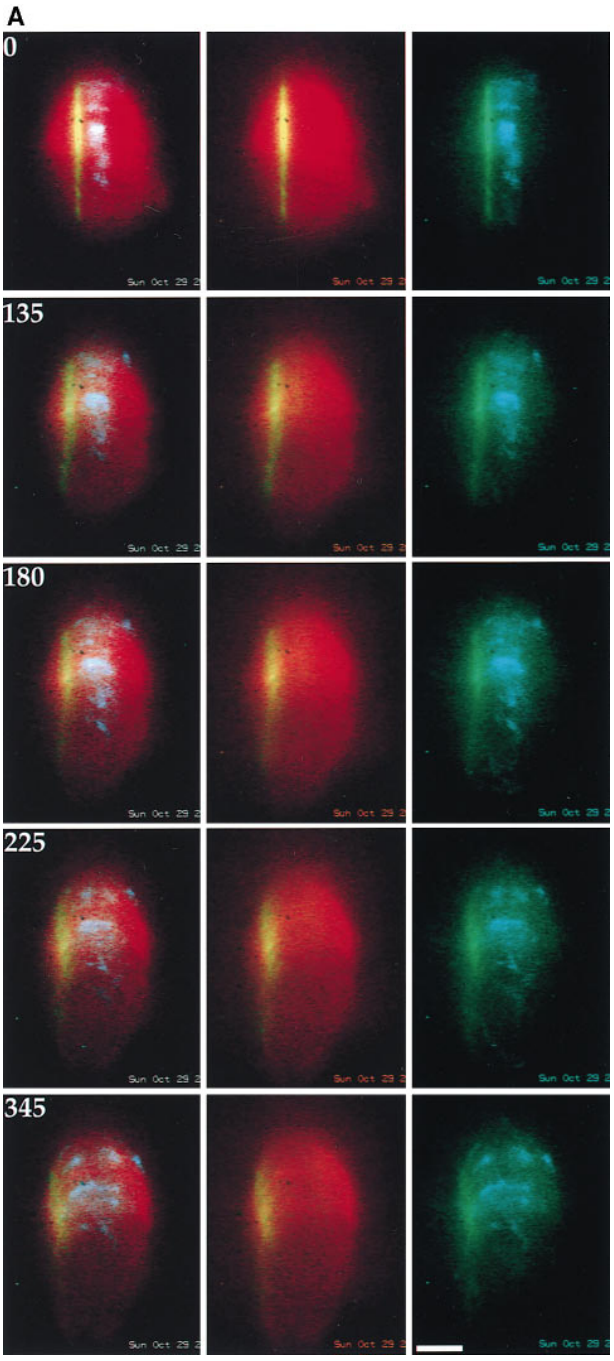

Figure 3. Simultaneous observation of chromosome movement and poleward MT flux in *Xenopus* extract spindles. (*A*) Panels from a sequence showing the similarity of poleward MT flux and chromosome movement during anaphase in *Xenopus* extract spindles. X-rhodamine tubulin-labeled spindle MTs are red, the photoactivated C2CF tubulin–containing MTs on the spindle MT lattice are green and the DAPI-labeled chromosomes are blue. The left column shows three-color overlays of the spindle, the mark and the chromosomes; the middle column shows two-color overlays of the fluorescent mark on the spindle MTs; and the right column shows two-color overlays of the chromosomes and the fluorescent mark. Time elapsed after the mark was made is indicated in seconds on the top left corner of the three-color overlay panels. For this particular sequence the mark was made 11 min after addition of calcium to trigger anaphase. (*B*) Fluorescence intensity linescan analysis of chromosome-to-pole movement and poleward MT flux during anaphase in *Xenopus* extract spindles. Fluorescence intensity along the spindle axis in the fluorescein channel is plotted for four different time points for the sequence in Fig. 3 *A*. The position of the leading edge of the chromosomes, obtained from linescans in the DAPI channel, is indicated by dots on the fluorescence intensity profiles of the mark. The left spindle pole is located at the x axis origin. The fluorescent mark, which was made close to the leading edges of the chromosomes, moved poleward and decayed in intensity, presumably as a result of spindle MT turnover. The mark also broadened as it moved, indicating the existence of differentially fluxing spindle MT subpopulations. (*C*) Summary of the analysis of rates of poleward MT flux (*F*) and chromosome-to-pole movement (*C*) during anaphase in *Xenopus* extract spindles. The plotted values represent the mean ± SD for rates measured on 11 spindles. Bar, 20 μm.

experiments performed on 11 spindles is shown in Fig. 3 *C*. After the onset of chromosome separation, chromosomes moved poleward at 2.2 ± 0.8 μm/min and MTs fluxed poleward at 2.0 ± 0.7 μm/min (mean ± SD for 11 spindles). These average rates were not significantly different ($P < 0.005$ in a *t* test). As the mark moved poleward, it both lost intensity and broadened, indicating the existence of faster and slower fluxing MT populations within the mark. Whereas the majority of segregating chromosomes did not move faster than the leading edge of the fluorescent mark, we occasionally observed short poleward movements by a few small chromosomes, well separated from the chromosomal mass, which were faster than the average flux rate (not shown).

Pharmacological Comparison of Anaphase Chromosome Movement and Poleward Microtubule Flux in Xenopus Extract Spindles

The similarity between the rate of chromosome movement and the rate of poleward MT flux during anaphase suggests that MT flux may be the predominant mechanism for chromosome-to-pole movement in *Xenopus* extract spindles. If this were true, then agents that inhibit MT flux should also inhibit chromosome-to-pole movement. In a previous study testing the effect of a variety of agents on poleward MT flux in *Xenopus* extract metaphase spindles, only AMPPNP was found to inhibit flux, blocking flux at a final concentration of 1.7 mM (Sawin and Mitchison,

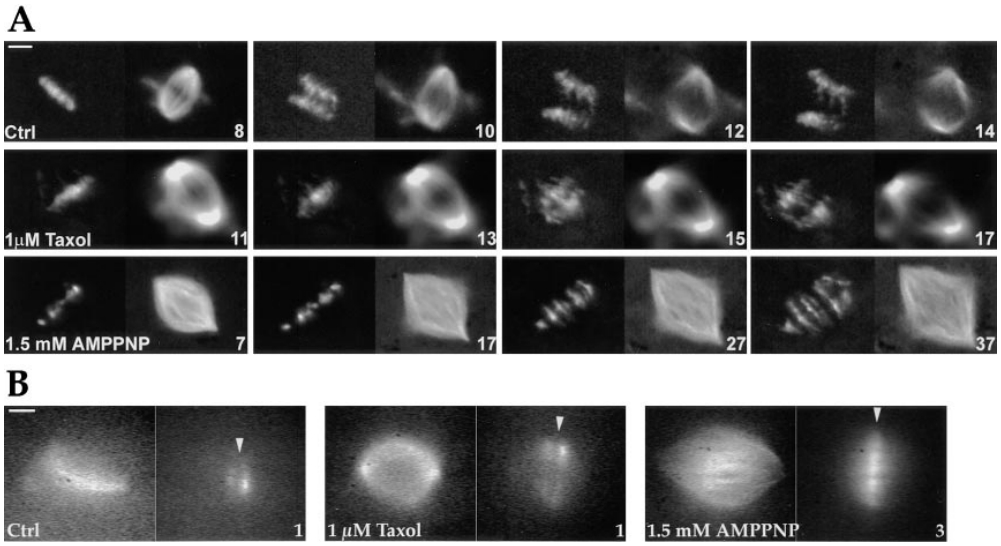

Figure 4. Pharmacological analysis of anaphase chromosome movement and poleward MT flux in *Xenopus* extract spindles. (*A*) Effect of taxol and AMPPNP treatments on chromosome movement and spindle structure during anaphase in vitro. Top row represents a control anaphase (*Ctrl*), the middle row represents anaphase in 1 μM taxol (*1 μM Taxol*), and the bottom row represents anaphase in 1.5 mM AMPPNP (*1.5 mM AMPPNP*). Taxol and AMPPNP were added along with the calcium used to initiate anaphase (t = 0 min). Each time point in the sequence is represented by paired DAPI-labeled chromosome (*left*) and X-rhodamine tubulin (*right*) images and the time after calcium addition is stamped in minutes on the lower right corner of the X-rhodamine tubulin image. Note both the much later times after calcium addition and the fivefold larger intervals (10 min vs. 2 min) between consecutive time points for the 1.5 mM AMPPNP sequence. The observed separation of sister chromatids in 1.5 mM AMPPNP is not due to chromosome-to-pole movement but primarily resulting from spindle elongation (see Fig. 5). (*B*) Effect of taxol and AMPPNP treatments on poleward MT flux. Paired X-rhodamine tubulin and fluorescein tubulin images are shown 1 min (for control and 1 μM taxol–treated spindles) and 3 min (for 1.5 mM AMPPNP–treated spindles) after the fluorescent mark was made on the spindle MTs. The initial position of the mark on the spindle is indicated by a white arrowhead. The 1 μM taxol spindle was marked 8 min after taxol addition. The 1.5 mM AMPPNP spindle was marked ~10 min after addition of calcium and AMPPNP. Bar-splitting occurs as a result of poleward flux of MTs emanating from opposite spindle poles (Sawin and Mitchison, 1991). The similar extent of splitting of the initially central fluorescent mark is evident in both the control and taxol-treated spindles. Significant bar-splitting is not evident in the presence of 1.5 mM AMPPNP. Even at much later times (up to 10 min after marking the spindle), there is no significant bar-splitting at this AMPPNP concentration (see also Sawin and Mitchison, 1991). Bars: (*A*) 20 μM; (*B*) 10 μm.

1991). Therefore, to test the prediction that AMPPNP would also inhibit chromosome movement, we analyzed anaphase chromosome movement at three AMPPNP concentrations: 0.5, 1, and 1.5 mM. We found that AMPPNP inhibited the rate of chromosome-to-pole movement in a dose-dependent manner (Fig. 4 *A*, *bottom row*; Figs. 5 *C*, and 6 *A*). We also confirmed that AMPPNP inhibited poleward MT flux by independently analyzing the effect of AMPPNP on MT flux in anaphase (Figs. 4 *B*, and 6 *B*). Since the chromosome movement and flux measurements were performed in separate experiments on different extract preparations and under different experimental conditions, the rates of the two processes are not directly comparable.

To address the concern that AMPPNP inhibition of chromosome movement had little to do with flux but was an indirect result of inhibiting exit from metaphase, we measured cdc2–cyclin B kinase activity after calcium addition in the absence or presence of varying amounts of AMPPNP. cdc2–cyclin B kinase activity, as measured by histone H1 phosphorylation, decays to interphase levels about 10–12 min after calcium addition in untreated extracts (Shamu and Murray, 1992). We found that AMPPNP did not inhibit exit from metaphase but delayed the drop in H1 kinase activity by ~3 min at 0.5 mM, 6 min at 1 mM, and 11 min at 1.5 mM (data not shown; n = 2 experiments with kinase assays performed at 2-min intervals for 30 min after calcium addition). This AMPPNP-induced delay in exit from metaphase is too short to account for the observed inhibition of chromosome-to-pole movement (see Fig. 4 *A*, comparing *top* and *bottom rows*). In addition, our analysis of chromosome movement in AMPPNP takes into consideration this delay, since chromosome position was tracked until "karyomere-associated motility" was apparent on the filmed spindles. Karyomere-associated motility is the rapid motility of decondensing chromosomes with nuclear envelopes (karyomeres) towards centers of MT asters, that has been previously shown to occur after anaphase A and to require inactivation of cdc2–cyclin B kinase activity (Murray et al., 1996). Consistent with the results of the H1 kinase assays, karyomere-associated motility was also delayed in the AMPPNP-treated spindles.

AMPPNP also did not appear to inhibit sister chromatid separation, since separated sisters were visible on some of the analyzed spindles after being moved apart by spindle expansion (Fig. 4 *A*, *bottom row*). That the observed separation of sister chromatids in 1.5 mM AMPPNP is not due to chromosome-to-pole movement but because of spindle expansion is demonstrated by tracking the position of the spindle poles and of the chromosomes as a function of time (Fig. 5 *C*).

In some of the spindles treated with 1.5 mM AMPPNP, we observed a small number of chromosomes (six chromosomes from five spindles in 1.5 mM AMPPNP) that appeared to be well separated from the chromosomal mass and moved short poleward distances at rates significantly faster than those for the bulk chromosomal mass (average

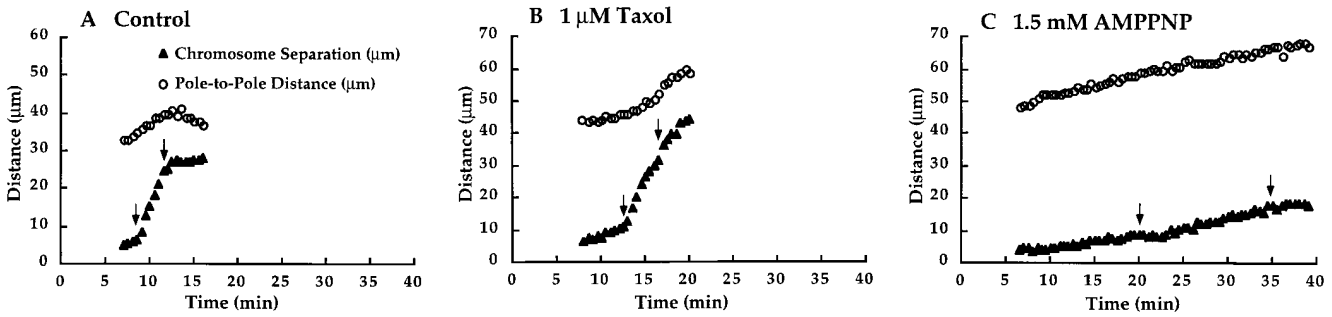

Figure 5. Anaphase kinetics of chromosome separation and spindle elongation in (*A*) control, (*B*) 1 μM taxol, and (*C*) 1.5 mM AMPPNP. Chromosome separation was measured as the distance (in μm) between the leading edges of separating sister chromatids as described (Murray et al., 1996). The arrows mark the region used to calculate the chromosome-to-pole movement rates after subtracting out the contribution from spindle elongation. Time 0 is when calcium was added to initiate anaphase. The rapid spindle elongation after chromosome separation in 1 μM taxol and the reduction in pole-to-pole distance after chromosome separation in the control sequence occur as a consequence of cytoplasmic flows in the extract moving the separated half spindles. There is no significant chromosome-to-pole movement in 1.5 mM AMPPNP for this particular spindle. These traces are for the sequences shown in Fig. 4 *A*.

rate of 0.6 μm/min; maximum rate of 0.8 μm/min versus average rate of 0.15 μm/min; maximum rate of 0.25 μm/min for the bulk chromosomal mass). These faster chromosomes moved at a third of the control rates of chromosome movement (~2 μm/min), but significantly faster than expected from the independently measured average flux rate (0.25 μm/min). Each spindle contains at least 18 chromosomes, with many spindles containing >18 as a result of lateral fusion of single sperm nucleus spindles. The faster moving chromosomes represent a small percentage (<5%) of the total number of observed chromosomes.

Taxol treatment of somatic newt lung cells during anaphase rapidly reduces the rate of chromosome-to-pole movement approximately fivefold. This occurs because taxol rapidly blocks MT assembly/disassembly at the kinetochore, inhibiting the "Pacman" kinetochore mechanism for anaphase A that predominates in these cells. Chromosomes continue moving poleward at the slow kMT flux rates, because taxol does not initially block poleward MT flux (Waters et al., 1996). These results predict that, if poleward MT flux is the predominant mechanism for anaphase chromosome movement in *Xenopus* extract spindles, then taxol should have little effect on anaphase A velocity in this system. To test this hypothesis, we analyzed anaphase chromosome movement in *Xenopus* extract spindles in the presence of 0.1, 0.5, 1, and 2 μM taxol. At 1 and 2 μM, taxol did not affect the rate of chromosome-to-pole movement even though it greatly increased the MT density near the spindle poles (Fig. 4 *A*, *middle row*; Figs. 5, and 6 *A*). The separated chromosomes migrated at control rates to the edge of this dense mass of MTs. Treatment with higher taxol concentrations (5 μM) was not possible because of the formation of taxol–tubulin aggregates throughout the extract. We also confirmed that 1 μM taxol did not significantly affect the rate of poleward MT flux in metaphase *Xenopus* extract spindles (Figs. 4 *B*, and 6 *B*). Analysis of the effect of taxol on MT flux was performed on metaphase spindles because the combination of the exit from metaphase and the taxol treatment greatly perturbed anaphase spindle structure, making marking experiments very difficult. The similar effects of taxol on MT flux during both metaphase and anaphase in somatic cells suggests that the sensitivity of the flux machinery to taxol does not change between metaphase and anaphase (Waters et al., 1996). We found that at longer times after addition of taxol (>30 min) metaphase spindles possessed extremely dense MT asters near the spindle poles and very weak MT density in the spindle midregion. Marks made at the edge of the very dense zone moved poleward slowly at <1 μm/min (not shown). Although the complex kinetic effects of taxol treatment remain to be explored, in the time and place that most anaphase chromosome movement occurs (between 5 and 15 min after the addition of taxol and from the middle of the spindle to the edge of the dense MT asters), chromosome-to-pole movement and poleward MT flux were unaffected.

In addition to poleward MT flux, a different type of minus end-directed poleward transport has been described recently in *Xenopus* extract spindles (Heald et al., 1996, 1997). When added to extracts, short fluorescently labeled MTs were found to move poleward with their minus end leading at average rates of ~6 μm/min, three times faster than anaphase chromosome movement. This poleward transport of short MTs was unaffected by addition of 2.5 mM AMPPNP but was inhibited by addition of either vanadate, which is known to inhibit cytoplasmic dynein motor activity, or an anti-cytoplasmic dynein intermediate chain monoclonal antibody (Heald et al., 1996, 1997). These results suggest that cytoplasmic dynein is responsible for the observed transport. To test if this dynein-dependent poleward transport plays any role in anaphase chromosome movement, we monitored anaphase in the presence of 25 or 50 μM vanadate. Although vanadate often accelerated spindle dissolution during anaphase (not shown), we did not find a significant effect of vanadate addition at these concentrations on the rate of chromosome-to-pole movement (Fig. 6 *A*). Rapid spindle dissolution during anaphase in the presence of vanadate prevented us from determining the effect of vanadate on anaphase poleward MT flux. However, cytoplasmic dynein does not appear to play a major role in poleward MT flux since neither treatment with 50–150 μM vanadate (Sawin and Mitchison, 1991) nor addition of p50dynamitin, a specific inhibitor of cytoplasmic dynein function (Echeverri et al., 1996), has a

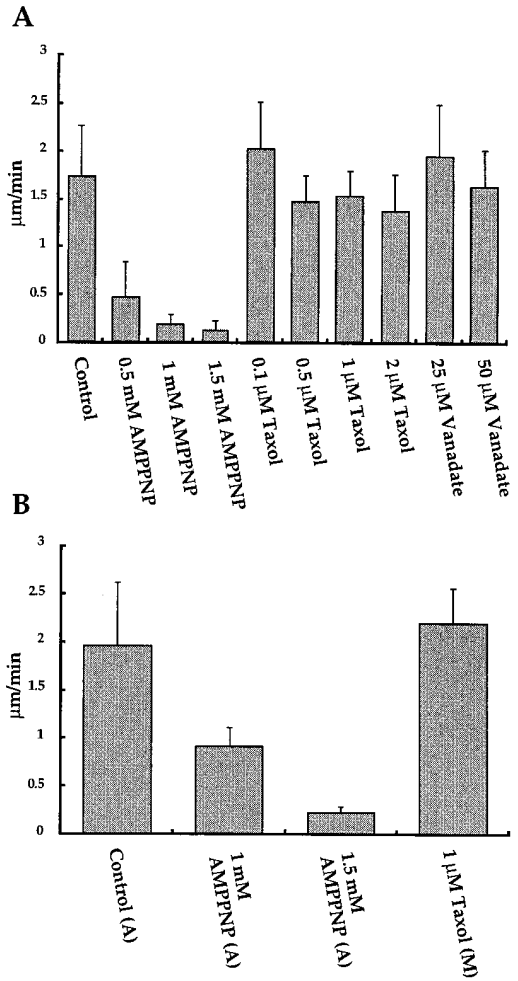

Figure 6. Summary of the analysis of the rates of chromosome-to-pole movement (*A*) and poleward MT flux (*B*) for the indicated treatments. The anaphase poleward MT flux value is replotted from Fig. 3 *C*. The experiments summarized here were performed on 13 different extract preparations. For the analysis of chromosome-to-pole movement a total of 65 sequences were acquired, of which 35 were analyzed to generate the data shown in *A*. Each condition represents analysis of chromosome movement on three to five spindles, with the exception of 25 μM vanadate (two spindles) and 2 μM taxol (two spindles). Multiple measurements were often performed on single spindles and the observed effects were qualitatively confirmed in both sequences that were not analyzed because of extensive flow-driven movements and fixed images acquired throughout the sample preparation at the end of each sequence. The flux measurements were made for six spindles in 1 mM AMPPNP, four spindles in 1.5 mM AMPPNP, and six spindles in 1 μM taxol. The analysis of the effect of AMPPNP on flux was done on anaphase (*A*) spindles whereas that of taxol on flux was done on metaphase (*M*) spindles.

significant effect on flux in metaphase *Xenopus* extract spindles (Shirasu, M., unpublished results).

Poleward Forces Act on Kinetochores during Metaphase in Xenopus Extract Spindles

Since poleward MT flux occurs during both metaphase and anaphase in *Xenopus* extract spindles, we looked for evidence of a poleward force acting on kinetochores during metaphase. In the in vitro spindles, chromosome arms are normally confined to a narrow equatorial region at metaphase (Figs. 2, and 7 *A*). However, unlike in somatic cells, the chromosomes on the in vitro spindles do not oscillate (not shown), indicating that the in vitro kinetochores do not exhibit directional instability. Thus, it was possible that poleward forces at kinetochores occur only after activation of anaphase in *Xenopus* extract spindles. Evidence that there is a poleward force on kinetochores during metaphase came from the morphology of chromosomes after spindles were held for 4–8 h in CSF metaphase arrest. Over this period, chromosome arms became partially disjoined and acrocentric centromere regions were seen extended poleward (Fig. 7 *B*). There was no detectable movement of the leading edges of the partially disjoined chromosomes over a 10-min period, indicating that poleward movement of the kinetochores was constrained by incomplete disjunction of the chromosome arms. Consistent with this hypothesis, small chromosomes were occasionally observed to move poleward at a rate similar to anaphase when they were no longer constrained by attachments near the metaphase plate (not shown). The prolonged metaphase-arrested spindles exhibited normal metaphase spindle morphology and retained anaphase competency since addition of a calcium pulse to these spindles activated the completion of chromosome disjunction and normal poleward chromosome movement (not shown).

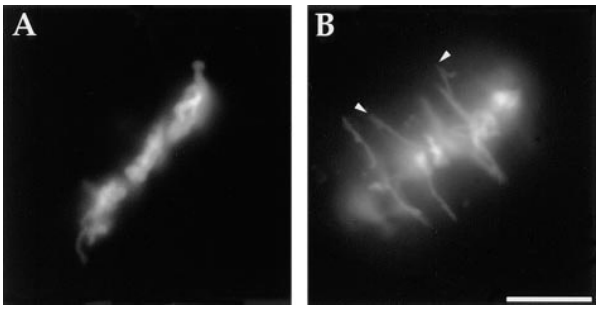

Figure 7. Morphology of chromosomes on *Xenopus* extract spindles in early metaphase arrest (*A*) and after a prolonged metaphase arrest (*B*). Arrowheads in *B* indicate the acrocentric centromere regions at the poleward edges of the partially disjoined chromosomes. This morphology was observed in experiments on several different extracts after a prolonged metaphase arrest. Bar, 10 μm.

Discussion

Anaphase A and Poleward Microtubule Flux Occur at Similar Rates in Xenopus Extract Spindles

Our anaphase marking experiments demonstrate that in *Xenopus* extract spindles the leading edge of the chromosomal mass moves poleward at the same average rate as a mark made on the spindle MTs (~2 μm/min). In contrast, kinetochores in vertebrate somatic cells move poleward during most of anaphase A at ~2 μm/min, whereas fluorescent marks on the kMTs flux poleward much more slowly at 0.3–0.5 μm/min (Mitchison and Salmon, 1992; Zhai et al., 1995). These results indicate that the "pole-

ward flux/traction fiber" model (Fig. 1 *B*) applies for anaphase A chromosome movement in spindles assembled in *Xenopus* extracts.

One caveat, when comparing MT marking experiments in *Xenopus* extract spindles to marking experiments in somatic cell spindles, is that MT populations detected by the marking procedure in the two systems are not the same. Marking experiments in somatic cell spindles detect primarily kMTs (Mitchison, 1989; Mitchison and Salmon, 1992; Zhai et al., 1995; Waters et al., 1996), whereas in *Xenopus* extract spindles they detect a large majority of the spindle MTs (Sawin and Mitchison, 1991). This difference most likely arises from the very different kMT/nonkMT (nonkinetochore microtubule) ratios in embryonic/meiotic versus somatic spindles and the much greater total number of MTs in the large embryonic spindles (Salmon and Segall, 1980; Sawin and Mitchison, 1991; Wise et al., 1991). Since in vitro spindle marking experiments are dominated by nonkMTs (Sawin and Mitchison, 1991, 1994), the conclusion from marking studies that poleward MT flux is the predominant mechanism for anaphase A chromosome movement rests on the untested assumption that kMTs and nonkMTs flux at the same rate. One way to avoid this assumption would be to determine the nonkMT flux rate in somatic cells, where the kMT flux rate is already known. However, the rapid turnover of nonkMTs has prevented a determination of their flux rate in somatic cells. Given our inability to distinguish kMTs from nonkMTs in *Xenopus* extract spindles, we have attempted to strengthen the conclusion from the marking experiment by comparing the response of anaphase A chromosome movement and poleward MT flux to treatment with different pharmacological agents.

Anaphase A and Poleward Microtubule Flux Exhibit Similar Responses to Pharmacological Perturbations in Xenopus Extract Spindles

If kinetochores and their associated chromosomes are pulled poleward primarily by MT flux, then inhibition of flux should inhibit anaphase A, whereas inhibition of MT disassembly at kinetochores should not inhibit anaphase A. An important finding in this study is that 1.5 mM AMPPNP, previously shown to inhibit flux (Sawin and Mitchison, 1991), inhibits anaphase A in the in vitro spindles. In contrast, microinjection of AMPPNP at final concentrations up to 5 mM in mitotic PtK1 cells does not substantially inhibit anaphase A, although it does strongly inhibit anaphase B (Lee, 1989). These results are consistent with an AMPPNP-insensitive Pacman kinetochore mechanism (Fig. 1 *A*) predominating during anaphase A in somatic cells versus an AMPPNP-sensitive poleward flux mechanism (Fig. 1 *B*) predominating during anaphase A in *Xenopus* extracts.

Interpretation of AMPPNP effects in extracts is complicated by the relative nonspecificity of this inhibitor. Several lines of evidence suggest that inhibition of poleward chromosome movement by AMPPNP is not due to inhibition of exit from metaphase or inhibition of chromosome disjunction. First, measurement of H1 kinase levels showed that AMPPNP did not inhibit exit from metaphase although it did delay the drop in H1 kinase activity in a dose-dependent manner. However, this delay was too short to account for the observed inhibition of chromosome-to-pole movement. Second, concentrations of AMPPNP higher than those used in our study did not inhibit either exit from metaphase or chromosome disjunction in PtK1 cells (Lee, 1989). Third, in the presence of AMPPNP, spindle pole-to-pole elongation revealed the presence of separated sisters on the in vitro spindles (Figs. 4 *A*, and 5 *C*).

The lack of an effect of taxol treatments on the rate of chromosome-to-pole movement is also consistent with poleward MT flux playing the predominant role during anaphase A in *Xenopus* extract spindles. This result was predicted from the effect of taxol on mitotic newt lung cells, where it does not immediately inhibit flux but does inhibit MT plus end assembly dynamics at the kinetochore and the component of anaphase A produced by kinetochores (Waters et al., 1996). Chromosome-to-pole movement at control rates in the presence of vanadate also excludes a significant role for dynein-dependent transport in anaphase chromosome movement in *Xenopus* extract spindles.

The combination of the marking studies and the pharmacology strongly suggest that MT flux plays a more dominant role in poleward chromosome movement in *Xenopus* extract spindles than in vertebrate somatic cells. However, in the AMPPNP treatments, as well as in control spindles, a small number of chromosomes moved significantly faster than the rest of the chromosomal mass and the independently measured average flux rate. These fast movements might represent either Pacman kinetochore activity or the latching of chromosomes onto a different type of poleward transport mechanism, such as the dynein-dependent transport of MT fragments (Heald et al., 1996, 1997). Alternatively, the faster movements may represent differentially fluxing MT subpopulations, the existence of which is indicated by spreading of the width of the fluorescent mark in both control (Fig. 3 *B*) and AMPPNP-treated spindles (Sawin and Mitchison, 1991).

Implications of Two Distinct Mechanisms for Anaphase A Chromosome Movement

It is tempting to speculate that anaphase A is produced primarily by Pacman kinetochore activity in cell types that have oscillating chromosomes, whereas a MT flux mechanism predominates in cell types that do not exhibit chromosome oscillations. In addition to *Xenopus* extract spindles, chromosome oscillations do not occur in spindles of insect spermatocytes (Forer, 1965, 1966; Nicklas, 1989), higher plants (Hard and Allen, 1977; Khodjakov et al., 1996), and echinoderm embryos (Ito et al., 1994*a,b*). Nicklas (1989) severed spindle fibers between the chromosomes and the pole of anaphase grasshopper spermatocytes and found that chromosome poleward movement persisted toward the severed ends of the fibers. From these results, Nicklas (1989) proposed that force generation for anaphase A is at or close to the kinetochore for this cell type. However, it is possible that the mechanisms that support/organize the poleward ends of the severed spindle fibers also produce poleward flux and minus end depolymerization. MT marking experiments using nonperturbing methods, like the fluorescence photoactivation

method used in our study, are urgently needed in these different systems to determine the generality of a predominantly poleward flux-driven mechanism for anaphase A.

Although it is possible that different cell types use fundamentally different mechanisms for anaphase A, we favor the idea that both mechanisms exist in all higher eukaryotic mitotic and meiotic spindles with one of them predominating during anaphase A (see also Mitchison and Salmon, 1992). We think this for the following reasons: (*a*) poleward MT flux makes a small but significant contribution to anaphase A in vertebrate somatic cells, where Pacman kinetochore movement predominates. Furthermore, in the later stages of anaphase A in newt lung cells, the kinetochores "park" on the MT lattice and are pulled poleward exclusively by MT flux (Mitchison and Salmon, 1992), much like kinetochores throughout anaphase A in *Xenopus* extract spindles; (*b*) kinetochores on *Xenopus* extract spindles, where poleward MT flux appears to predominate, recruit kinetochore components such as CENP-E, MCAK/XKCM1, and cytoplasmic dynein that are present at the kinetochores of somatic cells (Walczak et al., 1996; Desai et al., 1997; Wood et al., 1997). In addition, we saw limited evidence for occasional chromosome movement faster than the flux rate, possibly indicative of a Pacman contribution; and (*c*) in insect meiosis, where poleward movement of MT ablation zones at anaphase A rates argues for a predominance of the flux mechanism, analysis of acetylated tubulin distributions indicates that at least some depolymerization occurs at kinetochores during anaphase A (Wilson et al., 1994).

Why would many, perhaps all, cells have apparently redundant mechanisms for poleward chromosome movement? One possibility is that overlapping mechanisms provide a fail-safe system and increase the fidelity of segregation. Alternatively, both mechanisms play other roles in mitosis/meiosis, and may happen to overlap in moving chromosomes poleward. Specifically, we suspect that poleward MT flux, in addition to its role in moving chromosomes, is probably important in spindle assembly and may also help align chromosomes at the metaphase plate. MT dynamics at kinetochores, in addition to its role in moving chromosomes, may reflect the mechanisms used to attach MTs to kinetochores, and ensure bipolar orientation of chromosomes. In addition, motors at kinetochores may communicate with the checkpoint system (Nicklas, 1997; Rieder and Salmon, 1998) that proofreads this attachment using a tension sensor, which might be a motor itself.

We thank A. Murray for his role in starting this collaborative project and for his constant encouragement; S. Inoué and the Woods Hole Marine Biological Laboratory for providing laboratory space; the Marine Biological Laboratory (Woods Hole, MA) Physiology course for access to equipment; K. Oegema, C. Walczak, J. Swedlow, C. Waterman-Storer, and M. Shirasu for helpful comments on the manuscript.

This work was supported by grants from the National Institutes of Health to T.J. Mitchison and to E.D. Salmon (GM24364). A. Desai is a Howard Hughes Medical Institute pre-doctoral fellow.

Received for publication 9 December 1997 and in revised form 10 March 1998.

References

Desai, A., and T.J. Mitchison. 1998. Preparation and characterization of caged fluorescein tubulin. *Methods Enzymol.* In press.

Desai, A., H.W. Deacon, C.E. Walczak, and T.J. Mitchison. 1997. A method that allows the assembly of kinetochore components onto chromosomes condensed in clarified *Xenopus* egg extracts. *Proc. Nat. Acad. Sci. USA*. 94: 12378–12383.

Desai, A., A.W. Murray, T.J. Mitchison, and C.E. Walczak. 1998. The use of *Xenopus* egg extracts to study mitotic spindle assembly and function in vitro. *Methods Cell Biol.* In press.

Echeverri, C.J., B.M. Paschal, K.T. Vaughan, and R.B. Vallee. 1996. Molecular characterization of the 50-kD subunit of dynactin reveals function for the complex in chromosome alignment and spindle organization during mitosis. *J. Cell Biol.* 132:617–633.

Forer, A. 1965. Local reduction of spindle birefringence in living Nephrotoma suturalis (Loew) spermatocytes induced by ultraviolet microbeam irradiation. *J. Cell Biol.* 25:95–117.

Forer, A. 1966. Characterization of the mitotic traction system, and evidence that birefringent spindle fibers neither produce nor transmit force for chromosome movement. *Chromosoma (Berl.)*. 19:44–98.

Fuge, H. 1989. Traction fibres in chromosome movement: the pros and cons. *Biol. Cell.* 66:209–213.

Gorbsky, G.J., P.J. Sammak, and G.G. Borisy. 1987. Chromosomes move poleward in anaphase along stationary microtubules that coordinately disassemble from their kinetochore ends. *J. Cell Biol.* 104:9–18.

Gorbsky, G.J., P.J. Sammak, and G.G. Borisy. 1988. Microtubule dynamics and chromosome motion visualized in living anaphase cells. *J. Cell Biol.* 106: 1185–1192.

Graf, J.D., and H.R. Kobel. 1991. Genetics of *Xenopus laevis*. *Methods Cell Biol.* 36:19–34.

Hard, R., and R.D. Allen. 1977. Behaviour of kinetochore fibres in Haemanthus katherinae during anaphase movements of chromosomes. *J. Cell Sci*. 27: 47–56.

Heald, R., R. Tournebize, T. Blank, R. Sandaltzopoulos, P. Becker, A. Hyman, and E. Karsenti. 1996. Self-organization of microtubules into bipolar spindles around artificial chromosomes in *Xenopus* egg extracts. *Nature*. 382: 420–425.

Heald, R., R. Tournebize, A. Habermann, E. Karsenti, and A. Hyman. 1997. Spindle assembly in *Xenopus* egg extracts: Respective roles of centrosomes and microtubule self-organization. *J. Cell Biol*. 138:615–628.

Hyman, A., D. Drechsel, D. Kellogg, S. Salser, K. Sawin, P. Steffen, L. Wordeman, and T. Mitchison. 1991. Preparation of modified tubulins. *Methods Enzymol*. 196:478–485.

Inoué, S., and H. Sato. 1967. Cell motility by labile association of molecules. The nature of mitotic spindle fibers and their role in chromosome movement. *J. Gen. Physiol.* 50(Suppl.):259–292.

Ito, K., M. Masuda, K. Fujiwara, H. Hayashi, and H. Sato. 1994*a*. Metaphase and anaphase in the artificially induced monopolar spindle. *Proc. Nat. Acad. Sci. USA*. 91:3921–3925.

Ito, K., M. Masuda, K. Fujiwara, and H. Sato. 1994*b*. Do astral microtubules play a role in metaphase chromosome positioning? *Biol. Cell.* 82:95–102.

Khodjakov, A., R.W. Cole, A.S. Bajer, and C.L. Rieder. 1996. The force for poleward chromosome motion in Haemanthus cells acts along the length of the chromosome during metaphase but only at the kinetochore during anaphase. *J. Cell Biol*. 132:1093–1104.

Lee, G.M. 1989. Characterization of mitotic motors by their relative sensitivity to AMP-PNP. *J. Cell Sci.* 94:425–441.

Margolis, R.L., and L. Wilson. 1981. Microtubule treadmills--possible molecular machinery. *Nature*. 293:705–711.

Mitchison, T., L. Evans, E. Schulze, and M. Kirschner. 1986. Sites of microtubule assembly and disassembly in the mitotic spindle. *Cell*. 45:515–527.

Mitchison, T.J., K.E. Sawin, J.A. Theriot, K. Gee, and A. Mallavarapu. 1998. Caged Fluorescent Probes. *Methods Enzymol.* In Press.

Mitchison, T.J. 1989. Polewards microtubule flux in the mitotic spindle: evidence from photoactivation of fluorescence. *J. Cell Biol*. 109:637–652.

Mitchison, T.J., and E.D. Salmon. 1992. Poleward kinetochore fiber movement occurs during both metaphase and anaphase-A in newt lung cell mitosis. *J. Cell Biol*. 119:569–582.

Murray, A.W. 1991. Cell cycle extracts. *Methods Cell Biol*. 36:581–605.

Murray, A.W., A.B. Desai, and E.D. Salmon. 1996. Real time observation of anaphase in vitro. *Proc. Natl. Acad. Sci. USA*. 93:12327–12332.

Nicklas, R.B. 1989. The motor for poleward chromosome movement in anaphase is in or near the kinetochore. *J. Cell Biol*. 109:2245–2255.

Nicklas, R.B. 1997. How cells get the right chromosomes. *Science*. 275:632–637.

Rieder, C.L., and E.D. Salmon. 1994. Motile kinetochores and polar ejection forces dictate chromosome position on the vertebrate mitotic spindle. *J. Cell Biol.* 124:223–233.

Rieder, C.L., and E.D. Salmon. 1998. The vertebrate cell kinetochore and its roles in mitosis. *Trends Cell Biol*. In press.

Salmon, E.D. 1989. Microtubule dynamics and chromosome movement. *In* Mitosis: Molecules and Mechanisms. J. Hyams and B.R. Brinkley, editors. Academic Press, New York. 119–181.

Salmon, E.D., and R.R. Segall. 1980. Calcium-labile mitotic spindles isolated from sea urchin eggs (Lytechinus variegatus). *J. Cell Biol*. 86:355–365.

Salmon, E.D., T. Inoué, A. Desai, and A.W. Murray. 1994. High resolution multimode digital imaging system for mitosis studies in vivo and in vitro. *Biol. Bull.* 187:231–232.

Salmon, E.D., S.L. Shaw, J. Waters, C.M. Waterman-Storer, P.S. Maddox, E.

Yeh, and K. Bloom. 1998. A high resolution multimode digital microscope system. *Methods Cell Biol.* 56:185–215.
Sawin, K.E., and T.J. Mitchison. 1991. Poleward microtubule flux in mitotic spindles assembled in vitro. *J. Cell Biol.* 112:941–954.
Sawin, K.E., and T.J. Mitchison. 1994. Microtubule flux in mitosis is independent of chromosomes, centrosomes, and antiparallel microtubules. *Mol. Biol. Cell.* 5:217–226.
Shamu, C.E., and A.W. Murray. 1992. Sister chromatid separation in frog egg extracts requires DNA topoisomerase II activity during anaphase. *J. Cell Biol.* 117:921–934.
Wadsworth, P., and E.D. Salmon. 1986. Analysis of the treadmilling model during metaphase of mitosis using fluorescence redistribution after photobleaching. *J. Cell Biol.* 102:1032–1038.
Walczak, C.E., T.J. Mitchison, and A. Desai. 1996. XKCM1: a *Xenopus* kinesin-related protein that regulates microtubule dynamics during mitotic spindle assembly. *Cell.* 84:37–47.
Waters, J.C., T.J. Mitchison, C.L. Rieder, and E.D. Salmon. 1996. The kinetochore microtubule minus-end disassembly associated with poleward flux produces a force that can do work. *Mol. Biol. Cell.* 7:1547–1558.
Wilson, P.J., A. Forer, and C. Leggiadro. 1994. Evidence that kinetochore microtubules in crane-fly spermatocytes disassemble during anaphase primarily at the poleward end. *J. Cell Sci.* 107:3015–3027.
Wise, D., L. Cassimeris, C.L. Rieder, P. Wadsworth, and E.D. Salmon. 1991. Chromosome fiber dynamics and congression oscillations in metaphase PtK2 cells at 23 degrees C. *Cell. Motil. Cytoskeleton.* 18:131–142.
Wood, K.W., R. Sakowicz, L.S.B. Goldstein, and D.W. Cleveland. 1997. CENP-E is a plus end-directed kinetochore motor required for metaphase chromosome alignment. *Cell.* 91:357–366.
Yen, T.J., and B.T. Schaar. 1996. Kinetochore function: molecular motors, switches and gates. *Curr. Opin. Cell Biol.* 8:381–388.
Yen, T.J., G. Li, B.T. Schaar, I. Szilak, and D.W. Cleveland. 1992. CENP-E is a putative kinetochore motor that accumulates just before mitosis. *Nature.* 359:536–539.
Zhai, Y., P.J. Kronebusch, and G.G. Borisy. 1995. Kinetochore microtubule dynamics and the metaphase-anaphase transition. *J. Cell Biol.* 131:721–734.